Improving Point Cloud to Surface Reconstruction with Generalized Tikhonov Regularization

André F. R. Guarda
Instituto Superior Técnico
Instituto de Telecomunicações
Lisbon, Portugal
andre.guarda@lx.it.pt

José M. Bioucas-Dias
Instituto Superior Técnico
Instituto de Telecomunicações
Lisbon, Portugal
bioucas@lx.it.pt

Nuno M. M. Rodrigues
ESTG, Instituto Politécnico de Leiria
Instituto de Telecomunicações
Leiria, Portugal
nuno.rodrigues@co.it.pt

Fernando Pereira
Instituto Superior Técnico
Instituto de Telecomunicações
Lisbon, Portugal
fp@lx.it.pt

***Abstract* — Point cloud rendering has a vital role in the user Quality of Experience for applications adopting point cloud based representations. While this is not a new area, it has recently become more relevant with the recent interest on point cloud coding by major standardization groups, notably JPEG and MPEG. The screened Poisson surface reconstruction is a state-of-the-art technique for generating a watertight surface mesh from the point cloud samples. While its screening component allows the surface to better fit the cloud points, this fitting may lead to undesired artifacts in the surface, notably when the point cloud is noisy. This paper proposes to improve this reconstruction method by making it more robust to noise by adopting a generalized Tikhonov regularization term. The proposed regularization approach smooths regions that should be flat while keeping the important details in the edges, thus creating more pleasant surface reconstructions.**

Keywords — Point cloud rendering, surface reconstruction, generalized Tikhonov regularization, denoising

I. Introduction

Point clouds (PC) have recently emerged as a powerful format for the representation of 3D scenes, allowing their interactive visualization from virtually any viewpoint [1], [2], [3]. Point clouds represent the geometry of the scene as a set of points in a 3D coordinate system, as well as color information and other attributes for each point. Point cloud coding [4] is an emerging research area which is gaining the interest of international standardization groups like JPEG and MPEG as it has numerous applications, from real-time communication to virtual and augmented reality interaction [5].

However, since most available displays are still conventional 2D displays, it is necessary to render the 3D point cloud data into a 2D projection using some rendering algorithm. In this context, the rendering process becomes of utmost importance to offer high quality visual experiences, given that the end user will only see these resulting rendered images [6], [7], [8]. Because point clouds may involve a considerable amount of data, research for efficient lossy and lossless coding algorithms is very active [5]. In the point cloud processing pipeline, both the coding and rendering processes together determine the quality of the final user experience and thus the impact of rendering cannot be neglected, even because it cannot be simply avoided as it may happen for coding by using lossless or perceptually lossless coding solution.

A common class of methods to perform point cloud rendering consists in reconstructing a surface/mesh from the point cloud, and only then rendering the 2D images. Screened Poisson surface reconstruction (SPSR) [9], available in the Point Cloud Library (PCL) [10], is a state-of-the-art rendering technique that creates a watertight surface from the point cloud, which is represented by a 3D mesh. By using a screening term, acting as an interpolation constraint, the generated surface is encouraged to pass through the cloud points, thus achieving a high-fidelity reconstruction. However, as noted by the authors, when the input point cloud is noisy, this technique will create a surface that interpolates this noise, leading to undesirable reconstruction artifacts.

To mitigate this problem, this paper proposes the addition of a generalized Tikhonov (GT) regularization [11] term to the objective function adopted in [9]. This GT regularization, which is often used in image restoration applications, can be considered as a quadratic total variation. The use of this GT regularization makes the screened Poisson surface reconstruction method more robust to noisy point clouds, eliminating artifacts that would appear otherwise, while maintaining the detail of the reconstructed surface, thus achieving a better user Quality of Experience (QoE).

This paper is organized as follows: Section II introduces related work on point cloud rendering. Section III presents an overview of the screened Poisson surface reconstruction technique, while Section IV describes the proposed generalized Tikhonov regularization improvement and its implementation. Finally, Section V presents and discusses the obtained results, and Section VI concludes the paper.

II. Point Cloud Rendering: a Brief Review

Point cloud rendering techniques can be broadly grouped into two main categories: direct rendering and indirect rendering.

A. Direct Rendering

This type of techniques renders the 2D images directly from the point cloud data. The most straightforward method is to

This work was funded by Fundação para a Ciência e Tecnologia (FCT), Portugal, Ph.D. Grant SFRH/BD/118218/2016.

978-1-5090-3649-3/17/$31.00 ©2017 IEEE

project the 3D points into a 2D image; however, several issues may arise in the rendered image, such as holes (gaps between 2D pixels where 3D points are scarce) and the inappropriate projection of points that should be occluded for the rendered view point, i.e. points belonging to an object which is behind another object may still be projected and visible, even though they should not be visible.

Several methods for direct point cloud rendering involving splats have been proposed in the literature [12], [13], [14]. A splat is an ellipse or circle which is placed on a point and aligned with its tangent plane. In these rendering methods, splats are assigned to each point in the 3D (object) space, and are then projected into the 2D image (texture space). By using splats, these rendering methods fill the holes that would appear with a simple point projection. In addition, they also consider the occlusion issue by discarding the 3D points which belong to an occluded object (occlusion culling) or to the backside of an object (back-face culling), and thus are not visible anymore as desired.

Recently, MPEG has adopted a rendering software for its Point Cloud Compression (PCC) activity proposed by Technicolor [15]. In addition to points and splats, this solution can also use cubes placed in the points' locations, with selectable sizes, thus allowing some degree of hole filling. However, it does not take visibility culling into account.

While these methods may have low complexity in general, for high density point clouds with low shape complexity, i.e. for point clouds containing many points to represent simple surfaces that could be represented with much fewer points, the rendering of meshes can be advantageous.

B. Indirect Rendering

In this type of techniques, an intermediate 3D format, such as a mesh, is firstly obtained from the point cloud, and the 2D images are rendered from this intermediate format. A 3D mesh is a collection of vertices, edges and faces that defines the shape of an object; the faces usually consist of triangles (creating triangle meshes), quadrilaterals, or other simple convex polygons, since this simplifies the rendering process. The process of converting a point cloud to a mesh is essentially an inverse problem, where an approximation of the surface of the real object which is only represented with the given point samples has to be found.

The reconstruction of surfaces from oriented point samples, this means point clouds with normal associated to each point, has been a well-studied problem in computer graphics [16]. Some approaches involve interpolating most of the points to create a triangular mesh, using techniques such as Delaunay triangulation [17], [18], which are designated as combinatorial algorithms. However, as these techniques are typically susceptible to noise, a different type of approach using implicit functions has emerged. In this case, a 3D indicator function representing the object is initially obtained, and then the surface is extracted. The 3D indicator function has a value of zero on the surface, less than zero inside the object and greater than zero outside.

In [19], a Fourier transform-based reconstruction method is used. To compute the indicator function, its Fourier transform is firstly considered, in which the Fourier coefficients are determined by a volume integral of the indicator function. Using the Stokes' Theorem, this volume integral can be expressed as a surface integral, which solely depends on the points' positions on the surface and their respective normals, given as input data. Thus, the Fourier coefficients can be easily computed, and the indicator function is obtained by using the inverse Fourier transform. This method results in watertight surfaces.

A similar approach is proposed in [20], in which there is a connection between the indicator function of an object and the oriented points sampled from its surface (point cloud plus normals). In this case, the gradient of the indicator function is equal to the normal vectors at the surface of the object, as illustrated in Fig. 1. The problem of computing the indicator function can then be formulated as a Poisson equation, hence the name Poisson surface reconstruction, which is mathematically equivalent to the approach proposed in [19]; the two solutions yield similar results, with the advantage of lower complexity for the Poisson solution as it allows scalability. This method was later extended in [9] to include interpolation constraints, in order to achieve a tighter fitting of the reconstructed surface to the input point cloud. However, it loses robustness to noise, creating artifacts in the reconstructed surface for noisy point clouds. Nevertheless, this method is currently the state-of-the-art and it is available in the popular PCL software. As the solution proposed in this paper extends the so-called Screened Poisson surface reconstruction (SPSR) rendering solution [9], it will be presented with more detail in Section III.

III. Screened Poisson Surface Reconstruction: a Review

Poisson surface reconstruction is a method for reconstructing 3D surfaces from point clouds, which is based on an implicit function fitting approach. In this type of fitting approach, the indicator function defining the object is firstly computed, and then a mesh representing the surface is extracted using well-known methods.

Considering the gradient of this indicator function, it will be zero inside and outside the object, where the function is constant, while at the surface of the object it can be interpreted as a normal vector field. Thus, the point cloud with normals at its points corresponds to samples of this normal vector field (oriented point samples). The architecture of this rendering solution is shown in the top half of Fig. 2, and the various steps of this method are presented in the following.

A. Octree Discretization

Initially, the 3D space must be discretized for the representation of the indicator function. A traditional octree structure is used as it allows a high resolution near the points at the surface, while limiting the computational requirements. The 3D space is divided into 8 octants, and each octant containing points is recursively divided into smaller octants, until the desired octree depth is reached [21]. The octree is later enriched by adding nodes at coarser depths to allow a faster computation of the reconstruction algorithm.

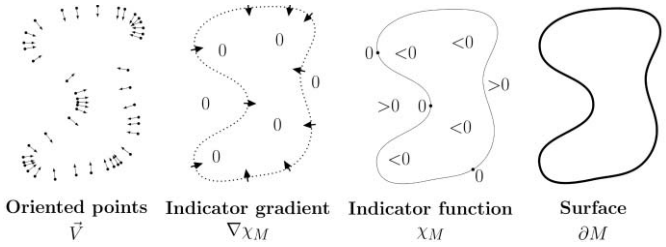

Fig. 1. 2D illustration of Poisson surface reconstruction [20].

B. Oriented Point Samples to Continuous Vector Field Transformation

To determine the object's indicator function, it is primarily required to obtain a continuous normal vector field from its original samples, i.e. the points with associated normals. With the 3D space discretized as an octree, a basis function $B_i,\ i \in [1, N]$ is associated to each octree node, typically a B-spline centered at each node and scaled according to its size. Then, the normal vector field $\overrightarrow{V}$ is represented as a linear combination of these B-splines and the normal vector of each point sample. Since point clouds can be sampled non-uniformly, the contribution of each sample is further filtered according to the sampling density at each point. That is, in regions with higher sampling density, each sample has a smaller weight.

C. Vector Field to Object Reconstruction

Given the normal vector field, $\overrightarrow{V}$, a 3D object has to be computed, represented by a volumetric indicator function χ, which has a zero value on the object's surface, less than zero inside the object and greater than zero outside. Furthermore, the indicator function gradient should correspond to the normal vector field ($\nabla\chi = \overrightarrow{V}$). Thus, the surface reconstruction problem may be formulated as the following variational problem:

$$\min_{\chi} \int \left\| \nabla\chi(q) - \overrightarrow{V}(q) \right\|^2 dq + \alpha \sum_{s\in S} \beta \|\chi(s)\|^2, \quad (1)$$

where $\|\ \|$ denotes the standard Euclidean norm, s is a point in the point cloud S, q is a point in the 3D space, α is the weight expressing the importance of fitting the point samples (screening term parameter), and β is a value depending on the point cloud sampling density. The second term corresponds to the screening term, which explicitly encourages the indicator function to have zero value at the sample (point cloud) positions, thus signaling that these points should belong to the surface. The minimum in (1) can then be obtained by solving a screened Poisson equation:

$$(\Delta - \alpha\tilde{I})\chi = \nabla.\overrightarrow{V}, \quad (2)$$

where Δ is the Laplacian and $\tilde{I}$ an appropriately defined operator. To transform the previous continuous equation into a finite dimensional system of equations, discretization is applied with respect to the previous basis functions B_i resulting into:

$$\langle (\Delta - \alpha\tilde{I})\chi, B_i \rangle = \langle \nabla.\overrightarrow{V}, B_i \rangle,\ i \in [1, N]. \quad (3)$$

The indicator function χ can also be expressed as a linear combination of the basis functions B_i as:

$$\chi(q) = \sum_{i=1}^{N} x_i B_i(q). \quad (4)$$

Thus, computing the indicator function sums up to finding the coefficients x_i in (4) by solving a linear system $Ax = b$, where

$$A_{ij} = \langle \nabla B_i, \nabla B_j \rangle + \alpha \langle \beta B_i, B_j \rangle \text{ and } b_i = \langle \vec{V}, \nabla B_i \rangle. \quad (5)$$

Since an octree was defined, this linear system is solved using a multigrid algorithm. B-splines are separated according to the depths of their corresponding nodes and a linear system is defined for each depth. The indicator function is then given by the sum of the solutions (coefficients x) for the linear systems for every depth, each affecting its corresponding B-spline.

D. Mesh Generation

After solving the previous system, a 3D object is obtained, represented as an indicator function. To generate a surface mesh from this 3D object, an isosurface (i.e. a surface representing points with the same value – isovalue) extraction method is applied. The zero value (per definition corresponding to the object surface) is selected as the isovalue to define the object surface. In the screened Poisson surface reconstruction, an adaptation of the Marching Cubes algorithm [22] is used to extract the isosurface.

IV. Improving Screened Poisson Surface Reconstruction

A major limitation of the screened Poisson surface reconstruction method reviewed in the previous section is the potential overfitting of the surface when the original point cloud is very noisy, leading to a surface with many artifacts. To mitigate this problem, this paper proposes a variation for the vector field to object reconstruction solution where a generalized Tikhonov regularization is performed at the finest level of the octree depth.

In this proposed modification, the multigrid algorithm described in Section III.C is used up to the last octree depth level, where the problem is then revisited to design a solution including a GT term. To solve the new regularization problem, a gradient descent method has been adopted. The architecture of the proposed improved regularization solution is presented in Fig. 2. The modifications regarding the original screened Poisson surface reconstruction method will be described in the next sections.

A. Generalized Tikhonov Regularization

The novel GT regularization approach adds a term to the surface reconstruction minimization problem that forces the smoothing of the indicator function [11]. However, since the reconstructed surface is obtained by extracting the isosurface with zero value, the edges and other details of the surface are preserved, while most of the noise is removed. By introducing a generalized Tikhonov regularization term in (1), the minimization problem becomes:

$$\min_{\chi} \int \left\| \nabla\chi(q) - \overrightarrow{V}(q) \right\|^2 dq + \alpha \sum_{s\in S} \beta \|\chi(s)\|^2 + \lambda\phi(\chi), \quad (6)$$

where λ is a regularization parameter expressing the weight attributed to the GT term given by:

$$\phi(\chi) = \sum_{s\in S} \sum_{o\in O(s)} |\chi(s) - \chi(o)|^2, \quad (7)$$

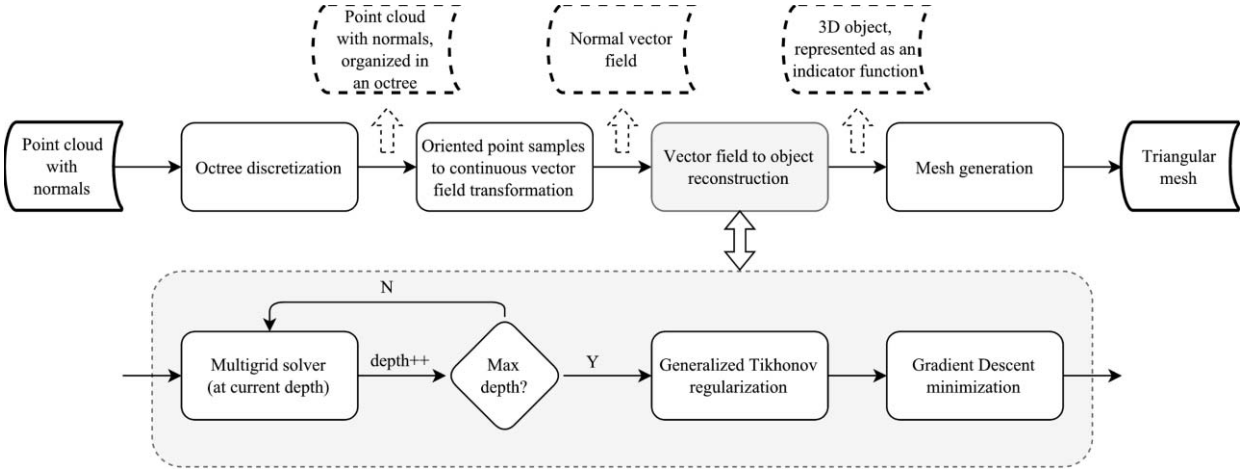

Fig. 2. Architecture of the improved screened Poisson surface reconstruction method, detailing the novel generalized Tikhonov regularization procedure.

where $O(s)$ are the existing adjacent neighboring nodes, up to 26 considering a 3×3×3 cube. Thus, the GT regularization is the norm of a gradient of the indicator function, and may be considered as a quadratic total variation. While in [23] a regularization method of similar form was presented to improve surface extrapolation where point data is missing, this GT regularization presents advantages in both extrapolation and denoising, due to the smoothing effect.

The minimization problem in (6) can be rewritten as:

$$\min_X \tfrac{1}{2}\|Y - H_1X\|^2 + \tfrac{1}{2}\alpha\|H_2X\|^2 + \\ + \lambda \sum_{s\in S}\sum_{o\in O(s)}|(C_s - C_o)^T X|^2, \quad (8)$$

where H_1, H_2, Y, X and C_s are matrices of suitable size, whose elements are: $H_{1_{ij}} = \langle \nabla B_i, \nabla B_j \rangle$, $H_{2_{ij}} = \langle \beta B_i, B_j \rangle$, $Y_i = \langle \vec{V}, \nabla B_i \rangle$, $X_i = x_i$ and $C_{s_i} = B_i(s)$. Solving (8) amounts to compute the solution of a large system of equations. This solution is obtained using the gradient descent optimization method.

B. Gradient Descent Minimization

Gradient descent is an iterative optimization method which generates a descent sequence $\hat{X}^{(i)}$, for $i = 1, \dots, iterations$, updating based on the information of the previous iteration [23]. However, the gradient descent method can take many iterations to converge to the minimum since it is a first order method [23]. As such, a Nesterov type accelerated gradient descent method was implemented instead, allowing a much faster convergence rate [23]. This has been done by updating the solution $\hat{X}^{(i)}$ not only with the information of the previous iteration $\hat{X}^{(i-1)}$ but also with the one of two iterations before $\hat{X}^{(i-2)}$, effectively becoming a second order method. The solution at iteration i of the gradient descent method is given by:

$$\hat{X}^{(i)} = Y^{(i-1)} - \gamma \nabla L(X)|_{\hat{X}^{(i-1)}}, \quad (9)$$

where γ is the step size, $\nabla L(X)|_{\hat{X}^{(i-1)}}$ is the gradient of the objective function evaluated for the solution at the previous iteration $i-1$, and

$$Y^{(i-1)} = \hat{X}^{(i-1)} + \tfrac{i-2}{i+1}\left(\hat{X}^{(i-1)} - \hat{X}^{(i-2)}\right). \quad (10)$$

The value for the step γ must be carefully selected as a too small value leads to a long convergence time while a large value may not lead to convergence. In [25] it is shown that, to guarantee convergence, the step γ is calculated such that $\gamma \leq \frac{1}{L}$, where L is the Lipschitz constant of the gradient of the objective function $\nabla L(X)$.

V. Performance Assessment

Several tests were designed to assess the performance of the SPSR method, with and without the proposed GT regularization term. The adopted test conditions are:

- **Point cloud datasets:** Statue Klimt, Egyptian mask, Frog67 and Head39 from the MPEG Call for Proposals for Point Cloud Compression [5].
- **Reconstruction parameters:** The PCL default parameters for the SPSR method have been used [10].

A. Screening Parameter α Impact

To set a reference benchmark for further tests, the original SPSR method [9] has been assessed using different values for its parameter α, notably 0, 1, 2, 4, 8 and 16; in this case, the GT regularization parameter λ is set to zero, thus it has no interference. The results for the Statue Klimt point cloud are shown in Fig. 3 and allow concluding:

- The resulting surface is very rugged, with a more prominent blob-like effect on the arms, face and hair of the woman, and child.
- As α increases, this effect is attenuated and the surface becomes more regular, i.e. it gives a better sense of the shape of the object and becomes more pleasant. This is explained by the fact that the screening term forces the surface to better fit the original points.
- However, some disturbing artifacts caused by point cloud outliers become more noticeable with the increase of α, as may be seen on the legs of the woman.

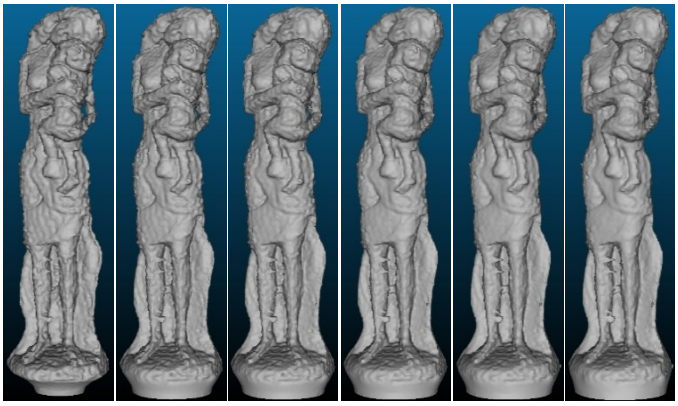

Fig. 3. Statue Klimt point cloud reconstructed with the SPSR method: from left to right, the screening parameter α takes values 0, 1, 2, 4, 8 and 16.

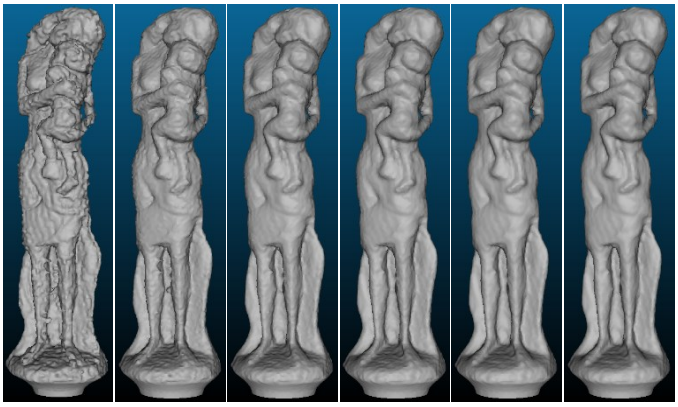

Fig. 4. Statue Klimt point cloud reconstructed with the proposed term: from left to right, the parameter λ takes values 0, 0.001, 0.005, 0.01, 0.05 and 0.1.

B. *Generalized Tikhonov Regularization Parameter λ Impact*

Now, the effect of the GT regularization term is studied by setting its parameter λ to a wide range of values, notably 0.001, 0.005, 0.01, 0.05 and 0.1; in this case, the screening parameter α is set to zero, thus the screening term has no impact on the reconstructed surface. The results for the Statue Klimt point cloud are shown in Fig. 4 and allow concluding:

- A stronger smoothing effect is present in comparison to the screening term impact, which allows eliminating most of the noise impact as well as the artifacts caused by outliers.
- This denoising feature is a well-known GT regularization attribute, namely the ability to smooth noisy flat regions. Since it is the indicator function that is smoothed, when extracting the isosurface the important edges are preserved.
- However, this smoothing comes at the price of some loss of details when λ is increased too much; for example, this is visible in the face of the woman and in legs of the child.
- Nonetheless, when comparing to the screening term results, the proposed GT regularization with λ=0.01 presents the best subjective performance of the previous tests.

C. *Combined Impact of α and λ Parameters*

Since the screening regularization term and the proposed GT regularization have distinctive features and reconstruction impacts, the joint use of both terms is evaluated, using combinations of the α and λ values previously tested. Fig. 5 and 0 show a comparison between the reconstruction results obtained with the reference method (with α=4), with the GT regularization only (λ=0.01), and with the proposed reconstruction method where the screening term and the novel generalized Tikhonov terms are combined with α=4 and λ=0.01. From these results, the following conclusions may be taken:

- With the proposed method, smoothing of flat regions is obtained while a high level of detail is still present. Artifacts caused by outliers have disappeared or have been greatly attenuated, due to the GT regularization term.
- The combination of both regularization terms achieves a denoising effect without compromising the details of the reconstructed object. This can be observed in the face of the woman and legs of the child in the Statue Klimt point cloud.
- Similarly, for Egyptian mask, Frog and Head point clouds, the surface obtained with the reference method presents noise artifacts such as a visible "wave" effect. This effect is mitigated with the proposed solution while preserving most of the detail, such as in the hair of Head or in the legs of Frog.

In summary, the proposed reconstruction method combining the two regularization terms is the best performing solution, allowing 'the best of both worlds', in a trade-off between presenting more detail and removing noise and outlier artifacts. However, the SPSR method is faster up to two orders of magnitude. Nevertheless, the best results for the tested point clouds were achieved with α=4 and λ=0.01. This type of advanced point cloud rendering is essential for the success of point cloud based content and associated applications.

VI. Conclusions

Screened Poisson surface reconstruction is a method for creating a mesh from a point cloud by computing an indicator function of the object from the point samples with normals. In this paper, a generalized Tikhonov regularization term was proposed to improve this surface reconstruction method.

The best subjective reconstruction results were achieved when the novel GT regularization term (λ=0.01) was combined with the screening term (α=4). Experimental results show a higher level of detail on the surface, while maintaining its smoothness, thus achieving more pleasant results. The proposed method has the added advantage of being robust to noise, including point cloud outliers. As future work, a more thorough evaluation will be completed, performing subjective tests with several people, using the mean opinion score to measure the performance of the proposed technique.

References

[1] G. Lafruit *et al.* , "Technical report of the joint ad hoc group for digital representations of light/sound fields for immersive media applications," Doc. MPEG N16352, Geneva, Switzerland, June 2016.

[2] C. Zhang, Q. Cai, P. A. Chou, Z. Zhang and R. M.-Brualla, "Viewport: A distributed, immersive teleconferencing system with infrared dot pattern," IEEE Multimedia, vol. 20, pp. 17-27, Jan.-Mar. 2013.

[3] C. Loop, C. Zhang and Z. Zhang, "Real-time high-resolution sparse voxelization with application to image-based modeling," in Proc. 5th High-Performance Graph. Conf., CA, USA, July 2013.

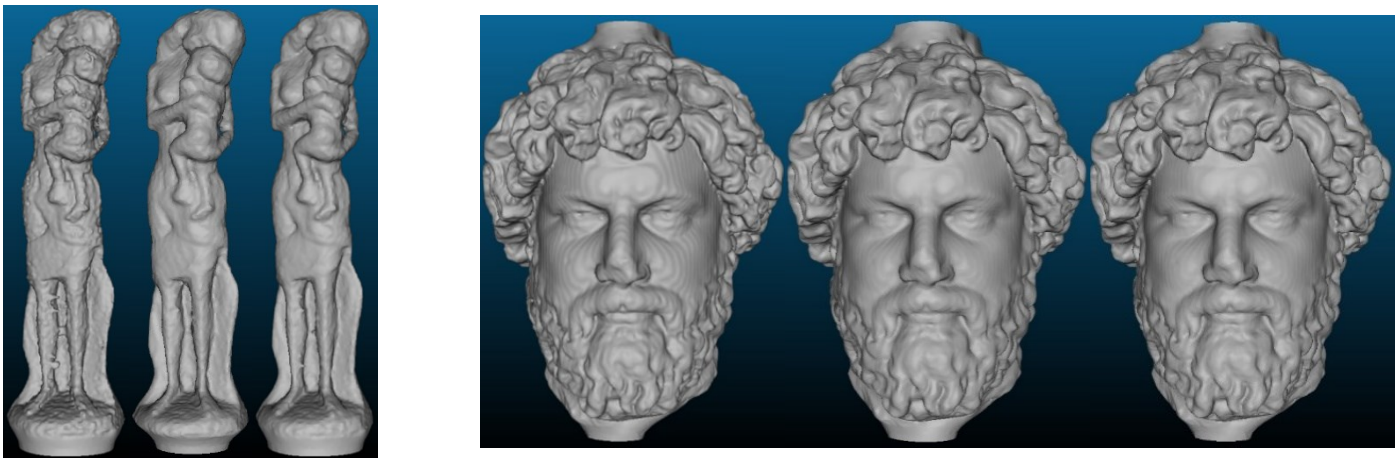

Fig. 5. Comparison of the reconstructed surfaces using the reference reconstruction method with α=4 (left), using only the GT regularization term λ=0.01 (middle) and the proposed solution combing the two regularization terms with α=4 and λ=0.01 (right), for Statue Klimt and Head39 point cloud datasets.

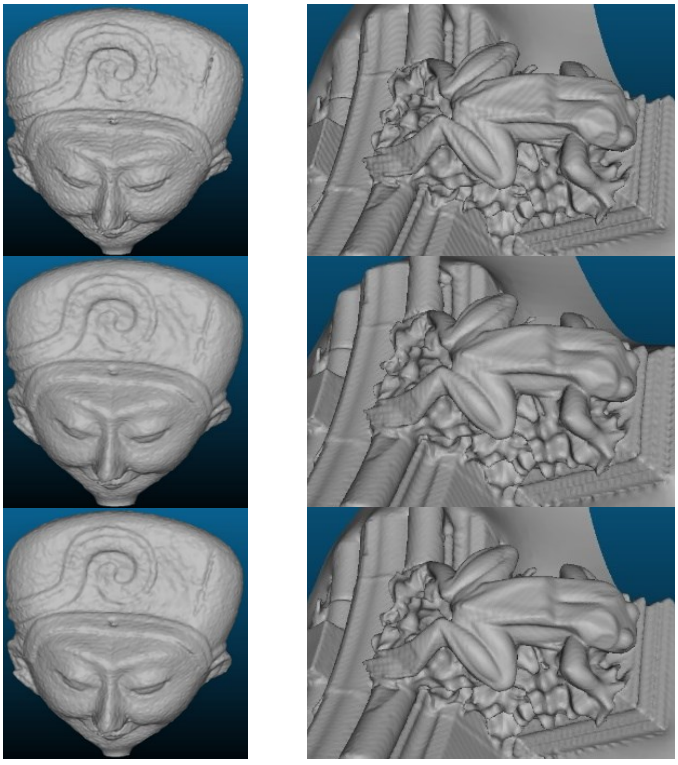

Fig. 6. Comparison of the reconstructed surfaces using the reference method with α=4 (top), using only the GT regularization term λ=0.01 (middle) and the proposed solution combing the two regularization terms with α=4 and λ=0.01 (bottom), for Egyptian mask and Frog67 point cloud datasets.

[4] Y. Huang, J. Peng, C.-C. J. Kuo and M. Gopi, "A generic scheme for progressive point cloud coding," Trans. Vis. Comput. Graphics, vol. 14, pp. 440-453, Mar.-Apr. 2008.

[5] "Call for proposals for Point Cloud Compression V2," Doc. MPEG N16763, Hobart, AU, Apr. 2017.

[6] H.-Y. Lin and Y.-H. Xiao, "Free-viewpoint image synthesis based on non-uniformly resampled 3D representation," in 17th IEEE Int. Conf. Image Process. (ICIP), Honk Kong, Sept. 2010.

[7] R. Tredinnick, M. Broecker and K. Ponto, "Progressive feedback point cloud rendering for virtual reality display," in IEEE Virtual Reality (VR), Greenville, SC, USA, Mar. 2016.

[8] H.-U. Kim *et al.*, "Hybrid representation and rendering of indoor environments using meshes and point clouds," in 11th Int. Conf. on Ubiquitous Robots and Ambient Intelligence (URAI), Kuala Lumpur, Malaysia, Nov. 2014.

[9] M. Kazhdan and H. Hoppe, "Screened Poisson Surface Reconstruction," ACM Trans. Graph., vol. 32, pp. 29:1--29:13, June 2013.

[10] S. Cousins and R. B. Rusu, "3D is here: Point Cloud Library (PCL)," in IEEE Int. Conf. Robot. Autom. (ICRA), Shanghai, China, May 2011.

[11] C. Vogel, "Computational Methods for Inverse Problems," SIAM, 2002.

[12] S. Rusinkiewicz and M. Levoy, "QSplat: A Multiresolution Point Rendering System for Large Meshes," in Proc. 27th Int. Conf. Comput. Graph. Interactive Techniques, New Orleans, LA, USA, July 2000.

[13] H. Pfister, M. Zwicker, J. van Baar and M. Gross, "Surfels: Surface Elements As Rendering Primitives," in Proc. 27th Int. Conf. Comput. Graph. Interactive Techniques, New Orleans, LA, USA, July 2000.

[14] M. Zwicker, H. Pfister, J. van Baar and M. Gross, "Surface Splatting," in Proc. 28th Int. Conf. Comput. Graph. and Interactive Techniques, Los Angeles, CA, USA, Aug. 2001.

[15] Documentation for Point Cloud Renderer, ISO/IEC JTC1/SC29 WG11 Doc. N16902, Hobart, AU, Apr. 2017.

[16] M. Berger *et al.*, "A Survey of Surface Reconstruction from Point Clouds," in Comput. Graph. Forum, vol. 36, pp. 301–329, Jan. 2017.

[17] J.-D. Boissonnat, "Geometric Structures for Three-dimensional Shape Representation," ACM Trans. Graph., vol. 3, pp. 266--286, Oct. 1984.

[18] R. Kolluri, J. R. Shewchuk and J. O'Brien, "Spectral Surface Reconstruction from Noisy Point Clouds," in ACM SIGGRAPH Symp. on Geometry Process., Nice, France, July 2004.

[19] M. Kazhdan, "Reconstruction of Solid Models from Oriented Point Sets," in Proc. 3rd Eurographics Symp. on Geometry Process., Vienna, Austria, July 2005.

[20] M. Kazhdan, M. Bolitho and H. Hoppe, "Poisson Surface Reconstruction," in Proc. 4th Eurographics Symp. on Geometry Process., Cagliari, Sardinia, Italy, June 2006.

[21] R. Schnabel and R. Klein, "Octree-based point-cloud compression.," in IEEE VGTC Conf. Point-Based Graph., Boston, MA, USA, July 2006.

[22] W. E. Lorensen and H. E. Cline, "Marching Cubes: A High Resolution 3D Surface Construction Algorithm," in Proc. 14th Int. Conf. Comput. Graph. and Interactive Techniques, Anaheim, CA, USA, July 1987.

[23] F. Calakli and G. Taubin, "SSD: Smooth Signed Distance Surface Reconstruction," in Comput. Graph. Forum, vol. 30, pp. 1993–2002, Sept. 2011.

[24] Y. Nesterov, Introductory Lectures on Convex Optimization: A Basic Course, Springer, 2004.

[25] D. P. Bertsekas, Nonlinear programming, 2nd ed., Belmont: Athena scientific, 1999.